Mononuclear Manganese(III) Complexes of a Heterodonor (N_2OS) Ligand containing Thiolate-type Sulfur: Synthesis, Structure, Redox and Spectroscopic Properties†

Sujit Baran Kumar,[a] Sudeep Bhattacharyya,[a] Subodh Kanti Dutta,[a] Edward R. T. Tiekink[b] and Muktimoy Chaudhury*[,a]

[a] *Department of Inorganic Chemistry, Indian Association for the Cultivation of Science, Calcutta 700 032, India*

[b] *Department of Chemistry, The University of Adelaide, Adelaide, South Australia 5005, Australia*

Two series of five-co-ordinate high-spin ($S = 2$) mononuclear manganese(III) complexes have been prepared of general formulae [MnL(X)] (X = Cl **1a**, Br **1b**, NCS **1c** or N_3 **1d**) and [MnL(B)]ClO_4 [B = pyridine (py) **2a**, 3-methylpyridine (3Me-py) **2b** or 4-methylpyridine (4Me-py) **2c**] using methyl 2-[2-(salicylideneamino)ethylamino]cyclopent-1-ene-1-carbodithioate (H_2L) as tetradentate ligand with a $(N_2OS)^{2-}$ donor set. The complexes have been characterised by a combination of IR and UV/VIS spectroscopy, magnetic measurements and electrochemical studies. Their UV/VIS spectra show two ligand-field transitions at *ca.* 685 ($^5B_1 \longrightarrow {}^5E$) and 570 nm ($^5B_1 \longrightarrow {}^5B_2$) along with a strong charge-transfer band in the near-UV region (*ca.* 440 nm), assigned as a phenolate $O \rightarrow Mn(d_\pi^*)$ ligand-to-metal charge-transfer transition. Cyclic voltammograms of the complexes (except **1d**) exhibit a one-electron quasi-reversible Mn^{III}–Mn^{II} reduction with $E_{\frac{1}{2}}$ close to −0.12 V (*vs.* saturated calomel electrode). For **1a–1c** irreversible Mn^{III}–Mn^{IV} oxidation is also observed. The compounds have an axially elongated square-pyramidal structure as dictated by the Jahn–Teller effect with ligands X or B occupying the axial position. Their electronic spectra and electrochemical properties show invariance with group X (or B) in the axial position. The crystal structure of complex **1b** was solved by Patterson and Fourier methods followed by a least-squares refinement to a conventional R value of 0.037. The basal plane of the five-co-ordinated manganese centre is defined by N (two), S and O atoms, derived from the ligand L. The co-ordinated S atom behaves like a thiolate anion as reflected by the C–S bond distance, 1.717(9) Å.

The resurgence of interest[1] in the co-ordination chemistry of manganese in recent years is a sequel to the recognition of its involvement in diverse biochemical processes associated with the metabolism of dioxygen and its reduced forms (O_2^{n-}). Enzymes catalysing these reactions need the obligatory presence of prosthetic groups containing manganese in the oxidation states ranging from +II to +IV with variable nuclearity.[2–4] The donor atom sets likely to be involved in co-ordination of Mn at these active centres are not known precisely. However, evidence in favour of N- and/or O-containing functionalities from amino acid side chains (histidine imidazole, tyrosine phenoxide, aspartate/glutamate carboxylate) is becoming increasingly prominent.[5] This has prompted several recent studies to generate higher-oxidation-state manganese chemistry at different nuclearity levels with ligands containing biologically relevant O/N donor sites. Some of the compounds reported lately[6–18] may be viewed as satisfactory models for the catalytic centres in a number of manganese enzymes.

Sugiura and co-workers[19] have reported the isolation and purification of a new manganese enzyme that displays acid phosphatase activity. A mononuclear manganese(III) centre bound by tyrosine phenolate and cysteine thiolate residues from within the protein is contemplated as the active site in this enzyme. Thus a sulfur-co-ordinated manganese centre, though still controversial,[20] is conceived for the first time in manganese biochemistry. One way of evaluating such a proposal is the synthesis of model manganese(III) compounds in a variety of co-ordination modes involving thiol as possible donor(s), the spectral and other properties of which can be compared to those of the proposed manganese biosite. Curiously, until now there have been only two reports[21,22] of structurally characterised mononuclear manganese(III) compounds containing exclusively biologically relevant heterodonor ligands with thiol sulfur in the donor site(s). One good reason for this is the reducing nature of the co-ordination environment, with thiol as possible donor considered not to be conducive in stabilising manganese in the +III oxidation state.[21–23]

As a part of our ongoing program on metal–sulfur chemistry[23,24] we have sought, therefore, to prepare such mononuclear manganese(III) complexes with sufficient stability for spectroscopic characterisation. In this paper we report some manganese(III) complexes containing methyl 2-[2-(salicylideneamino)ethylamino]cyclopent-1-ene-1-carbodithioate (H_2L) as the ligand in which[25] and in related compounds[26] the carbodithioate sulfurs behave more like thiolate anion in their metal-bound state as confirmed by X-ray diffraction analysis.[26] Two series of five-co-ordinated complexes [MnL(X)] **1a–1d** (X = unidentate anionic ligand) and [MnL(B)]ClO_4 **2a–2c** (B = nitrogen-containing heterocyclic base) have been prepared and their spectral, magnetic and electrochemical properties are reported. The crystal and molecular structure of a representative compound [MnL(Br)] **1b** is also reported.

† *Supplementary data available:* see Instructions for Authors, *J. Chem. Soc. Dalton Trans.*, 1995, Issue 1, pp. xxv–xxx.

Non-SI units employed: eV ≈ 1.60 × 10^{-19} J; $\mu_B \approx 9.27 \times 10^{-24}$ J T^{-1}.

Experimental

Materials.—The ligand H_2L[25] and the precursor compounds $Mn(O_2CMe)_3{\cdot}2H_2O$[27] and $[Mn(acac)_2(NCS)]$[28] were prepared as described in the literature. Cyclopentanone (E. Merck), ethylenediamine (BDH) and salicylaldehyde (Loba Chemie) were freshly distilled before use. Pyridine, 3-methyl- and 4-methyl-pyridine (3Me- and 4Me-py) (all from Aldrich) were purified by refluxing over anhydrous K_2CO_3 followed by distillation over an efficient fractionating column. Solvents were reagent grade, distilled from the appropriate drying agents[29] under nitrogen and degassed prior to use. All other chemicals were reagent grade available commercially and used as received.

Syntheses.—Preparations of the following compounds were carried out under an atmosphere of purified dinitrogen.

[MnL(Cl)] **1a**. A solution of H_2L (0.32 g, 1 mmol) in CH_2Cl_2 (15 cm^3) was added dropwise to a stirred solution of $Mn(O_2CMe)_3{\cdot}2H_2O$ (0.27 g, 1 mmol) in methanol (15 cm^3) under nitrogen. After 20 min of stirring, the solution was filtered. The filtrate was combined with an excess (0.22 g, 5 mmol) of LiCl in methanol (10 cm^3) and stirred for 1 h. A dark brown shining microcrystalline solid began to precipitate during this time. The solid was filtered off, washed with hexane and dried in vacuum. Recrystallisation can be effected from CH_2Cl_2–hexane. Yield: 0.27 g (65%) (Found: C, 47.1; H, 4.6; N, 7.1. $C_{16}H_{18}ClMnN_2OS_2$ requires C, 47.0; H, 4.4; N, 6.85%). IR (KBr disc): ν(C=N) 1615s, ν(C=C, phenyl ring) 1580s, ν(C⋯O) 1540s, ν(C⋯N + C⋯C) 1450s, ν(Mn–O) 630m, ν(Mn–N) 460, 420m and ν(Mn–S) 360m cm^{-1}.

[MnL(Br)] **1b**. This compound was prepared as above, but using LiBr instead of LiCl, in 50% yield (Found: C, 42.9; H, 4.0; N, 5.9. $C_{16}H_{18}BrMnN_2OS_2$ requires C, 42.4; H, 3.95; N, 6.2%). IR (KBr disc): ν(C=N) 1610s, ν(C=C, phenyl ring) 1590m, ν(C⋯O) 1535m, ν(C⋯N + C⋯C) 1440s, ν(Mn–O) 625s, ν(Mn–N) 450, 410m and ν(Mn–S) 350m cm^{-1}.

Crystals suitable for X-ray crystallographic analyses were obtained by slow diffusion of hexane into a CH_2Cl_2 solution of the compound.

[MnL(NCS)] **1c**. *Method A*. The procedure was identical to that for complexes **1a** and **1b** with the use of KSCN. The dark brown product thus isolated was recrystallised from CH_2Cl_2. Yield: 60%.

Method B. A green methanolic solution (15 cm^3) of $[Mn(acac)_2(NCS)]$[28] (Hacac = acetylacetone) (0.31 g, 1 mmol) was stirred for 3 h at room temperature with an equimolar amount of H_2L in CH_2Cl_2 (15 cm^3). The resulting deep brown solution was concentrated to *ca.* 20 cm^3 and left undisturbed for 1 h. A microcrystalline precipitate was then filtered off and recrystallised by slow evaporation from CH_2Cl_2. Yield: 0.31 g (72%) (Found: C, 47.2; H, 4.2; N, 9.8. $C_{17}H_{18}MnN_3OS_3$ requires C, 47.35; H, 4.2; N, 9.75%). IR (KBr disc): ν(C=N) 2060s, ν(C=N) + ν(C=C, phenyl ring) 1595s, ν(C⋯O) 1540s, ν(C⋯N + C⋯C) 1440s, ν(C=S) 800m, ν(Mn–O) 645m, ν(Mn–N) 470, 420m and ν(Mn–S) 350m cm^{-1}.

[MnL(N_3)] **1d**. To a stirred solution of $Mn(O_2CMe)_3{\cdot}2H_2O$ (0.27 g, 1 mmol) in degassed methanol (5 cm^3) was added dropwise a CH_2Cl_2 solution (10 cm^3) of H_2L (0.32 g, 1 mmol). After 10 min the resulting solution was filtered. The filtrate was combined with a concentrated solution of sodium azide in water containing slightly more than the equivalent amount of the anion, and left under stirring at room temperature for 0.5 h. The dark brown crystalline product was filtered off, washed with ethanol, dried in vacuum and finally recrystallised from CH_2Cl_2–hexane. Yield: 0.14 g (35%) (Found: C, 45.9; H, 4.5; N, 16.7. $C_{16}H_{18}MnN_5OS_2$ requires C, 46.25; H, 4.35; N, 16.85%). IR (KBr disc): $\nu_{asym}(N_3)$ 2040s, ν(C=N) 1615s, ν(C=C, phenyl ring) 1590m, ν(C⋯O) 1540m, ν(C⋯N + C⋯C) 1450s, ν(Mn–O) 620m, ν(Mn–N) 460, 410m and ν(Mn–S) 350m cm^{-1}.

[MnL(3Me-py)]ClO_4 **2b**. To a stirred suspension of complex **1a** (0.3 g, 0.7 mmol) in acetonitrile (15 cm^3) containing 3-methylpyridine (0.14 g, 1.5 mmol) was slowly added a solid sample of silver perchlorate (0.16 g, 0.75 mmol) in small portions. The complex dissolved as the reaction proceeded. After 3 h the solution was filtered to remove the precipitated silver chloride. The deep brown supernatant was concentrated to small volume (*ca.* 5 cm^3) under reduced pressure and then stored in a freezer overnight to yield dark brown crystals. The product was recrystallised from acetonitrile alone. Yield: 0.18 g (44%) (Found: C, 46.5; H, 4.6; N, 7.7. $C_{22}H_{25}ClMnN_3O_5S_2$ requires C, 46.7; H, 4.40; N, 7.45%). IR (KBr disc): ν(C=N) 1610s, ν(C=C, phenyl ring) 1590m, ν(C⋯O) 1530s; ν(C⋯N + C=C) 1440s, ν_{asym}(Cl–O) 1080s, δ(O–Cl–O) + ν(Mn–O) 620s, ν(Mn–N) 455, 440m and ν(Mn–S) 355m cm^{-1}.

[MnL(py)]ClO_4 **2a**. Pyridine (py) was used in place of 3-methylpyridine. The procedure was otherwise completely analogous to that for complex **2b**. Yield: 40% (Found: C, 45.5; H, 4.0; N, 8.1. $C_{21}H_{23}ClMnN_3O_5S_2$ requires C, 45.7; H, 4.15; N, 7.6%). IR (KBr disc): ν(C=N) 1610s, ν(C=C, phenyl ring) 1590s, ν(C⋯O) 1540m, ν(C⋯N + C⋯C), 1440s, ν_{asym}(Cl–O) 1085s, δ(O–Cl–O) + ν(Mn–O) 620s, ν(Mn–N) 460, 440m and ν(Mn–S) 355m cm^{-1}.

[MnL(4Me-py)]ClO_4 **2c**. This compound was prepared in 52% yield following essentially the same procedure as that for **2b** but from 4-methylpyridine (Found: C, 46.3; H, 4.4; N, 7.5. $C_{22}H_{25}ClMnN_3O_5S_2$ requires C, 46.7; H, 4.4; N, 7.45%). IR (KBr disc): ν(C=N) 1610s, ν(C=C, phenyl ring) 1590s, ν(C⋯O) 1535s, ν(C⋯N + C⋯O) 1440s, ν_{asym}(Cl–O) 1080s, δ(O–Cl–O) + ν(Mn–O) 625s, ν(Mn–N) 460, 440m and ν(Mn–S) 350m cm^{-1}.

The complexes [Mn(salen)(NCS)] [H_2salen = *N*,*N*′-bis(salicylidene)ethane-1,2-diamine], [Mn(acacen)(NCS)] [H_2-acacen = *N*,*N*′-bis(1-methyl-3-oxobutylidene)ethane-1,2-diamine], [Mn(msalen)(NCS)] [H_2msalen = *N*,*N*′-bis(2-methylsalicylidene)ethane-1,2-diamine] and [Mn(salophen)-(NCS)] [H_2salophen = *N*,*N*′-bis(salicylidene)-*o*-phenylenediamine] were prepared following the same procedure (Method A) as described for **1c** with the appropriate Schiff base but using MeCN as solvent for recrystallisation.

Physical Methods.—Elemental analyses (C, H and N), IR, UV/VIS spectra, solution electrical conductivity and magnetic measurements were performed as described elsewhere.[24] Electrochemical measurements were made with a BAS-100B electrochemical analyser. Cyclic voltammograms were recorded at 25 ± 1 °C in the designated solvent under dinitrogen with the electroactive component at *ca.* 10^{-3} mol dm^{-3}. Tetraethylammonium perchlorate (0.1 mol dm^{-3}) was used as the supporting electrolyte. A three-electrode configuration was employed with either a Ag–AgCl or saturated calomel electrode (SCE) as reference and platinum working and auxiliary electrodes. The electrode performance was monitored by observing the ferrocene couple. Bulk electrolyses were carried out with the use of a platinum-gauze working electrode. Scrupulously dried and freshly distilled deoxygenated solvents were used throughout. Potentials are reported relative to the SCE, uncorrected for junction potentials.

X-Ray Crystallography.—Intensity data for complex **1b** (0.17 × 0.17 × 0.35 mm) were measured on a Rigaku AFC6R diffractometer equipped with graphite-monochromatized Mo-Kα radiation, λ = 0.710 73 Å; the ω-2θ scan technique was employed to measure data up to a maximum Bragg angle of 27.5°. The data set was corrected for Lorentz and polarisation effects[30] and an empirical absorption correction was applied such that the range of transmission factors was 0.956–1.098.[31] Crystal data are given in Table 2.

The structure was solved by direct methods[32] and refined by a full-matrix least-squares procedure based on *F*.[30] Non-H atoms were refined with anisotropic thermal parameters and H atoms were included in the model in their calculated positions

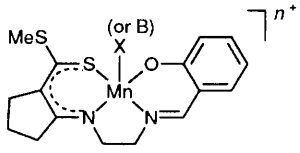

n = 0; X = Cl, Br, NCS, or N_3
n = 1; B = py, 3Me-py or 4Me-py

Table 1 Molar conductances[a] and magnetic moments[b] of the complexes

Complex	Molar conductance: Solvent	Λ_M/S cm^2 mol^{-1}	μ_{eff}/μ_B
1a	dmf	58	4.89
	Nitrobenzene	—	
1b	dmf	53	4.90
	Nitrobenzene	—	
1c	dmf	62	4.88
	Nitrobenzene	—	
1d	dmf	68	4.71
	Nitrobenzene	—	
2a	dmf	63	4.87
	Nitrobenzene	26	
2b	dmf	56	4.83
	Nitrobenzene	21	
2c	dmf	63	4.84
	Nitrobenzene	28	

[a] Measured for *ca.* 10^{-3} mol dm^{-3} solutions at 25 °C. [b] Powdered polycrystalline samples at 25 °C.

(C–H 0.97 Å). The refinement was continued until convergence employing sigma weights; the analysis of variance showed no special features indicating that an appropriate weighting scheme had been applied. The absolute configuration of the crystal was determined on the basis of the refinement of the opposite hand which yielded markedly higher residuals. Final values for R and R' were 0.037 and 0.038, respectively; the fractional atomic coordinates are listed in Table 3 and the numbering scheme employed is shown in Fig. 1 (drawn using ORTEP[33] with 25% probability ellipsoids). Selected bond distances and angles are given in Table 4. The TEXSAN[30] package, installed on an Iris Indigo workstation, was employed in all calculations.

Additional material available from the Cambridge Crystallographic Data Centre comprises H-atom coordinates, thermal parameters and remaining bond lengths and angles.

Results and Discussion

[MnL(X)] *Complexes* **1a**–**1d**.—The reaction of $Mn(O_2CMe)_3 \cdot 2H_2O$ in methanol with the stoichiometric amount of H_2L (1 : 1 mol ratio) in the presence of the appropriate mononegative anion (X) added in large molar excess yields crystalline compounds **1a**–**1d** in yields of 35–72%. These are air-stable intense dark solids having varying degrees of solubility in common organic solvents. In solution, with the exception of **1d**, they are all stable for extended periods of time.

The IR spectra (KBr disc) of the complexes have several prominent features. The medium-intensity ν(N–H) vibration, appearing at 2930 cm^{-1} in the spectrum of free H_2L, is totally absent in the spectrum of the complexes: this provides explicit evidence for a co-ordinated amino nitrogen atom. Further comparison with the spectrum of free H_2L reveals the presence of a strong band in the spectra of the complexes at *ca.* 1540 cm^{-1} due to the ν(C⋯O) stretch of the phenolate anion, providing convincing evidence of its participation in the metal–ligand bonding (see below). Additional strong absorptions at *ca.* 1610, 1590 and 1440 cm^{-1}, typical of the co-ordinated ligand L, have been previously assigned to ν(C=N), ν(C=C, phenyl ring) and ν(C⋯N + C⋯C) stretching modes respectively.[25] The appearance of a strong ν(C=N) stretch at 2060 cm^{-1} coupled with a medium-intensity ν(C=S) absorption appearing at 800 cm^{-1} for **1c** are indicative of N-bonded isothiocyanate.[34] Also a sharp strong band at 2040 cm^{-1} in **1d** due to the azide antisymmetric stretch $\nu_{asym}(N_3)$ provides evidence in favour of an azide bonding.[35] Thus, the ligand is dianionic in complexes **1a**–**1d** and, as shown below, forms the square base of a five-co-ordinated square-pyramidal (C_{4v}) molecule using both nitrogen atoms, the phenoxide oxygen and carbodithioate sulfur with grossly thiolate character as confirmed by X-ray crystallography (see below).

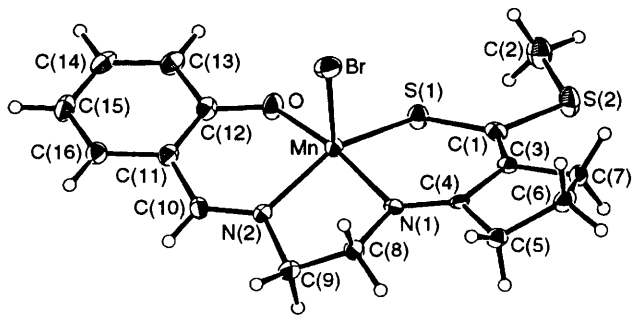

Fig. 1 Molecular structure and atom numbering of the non-hydrogen atoms (25% probability thermal ellipsoids) of [MnL(Br)] **1b**

Electrical conductivity measurements in nitrobenzene solution at *ca.* 10^{-3} mol dm^{-3}, determined at 25 °C, indicate that the complexes are uncharged, existing as discrete molecules with the anion (X) remaining intact in the apical position. By contrast, in dimethylformamide (dmf) the conductivity values are in the range 53–68 S cm^2 mol^{-1} (Table 1) close to the expected limit[36] for a 1 : 1 electrolyte and providing evidence for extensive anion dissociation in this co-ordinating solvent.

Crystal and Molecular Structure of [MnL(Br)] **1b**.—The crystal structure determination of complex **1b** confirms the stoichiometry and is consistent with the spectroscopic results (see below) and thereby serves as a prototype for the [MnL(X)] structures described above. The molecular structure of **1b** (Fig. 1, Tables 2–4) is comprised of discrete molecules, there being no significant intermolecular contacts in the lattice; the closest non-hydrogen contact of 3.36(1) Å occurs between the C(4) and C(14) atoms (symmetry operation: $-\frac{1}{2} + x, -\frac{1}{2} + y, z$). The Mn atom exists in a distorted square-pyramidal geometry with the four basal positions being occupied by an S, two N and the O atoms derived from the dinegative, tetradentate ligand L. The axial site is occupied by the Br atom which forms angles in the range 91.2(2)–111.32(8)° with the basal plane. The lack of symmetry in the molecule confirms the choice of the space group as *Cc*.

The C(1)–S(1) bond distance of 1.717(9) Å is not experimentally distinct from C(1)–S(2) 1.740(8) Å and this, coupled with the relatively short Mn–S(1) separation 2.271(2) Å, provides evidence that atom S(1) functions as a thiolate donor. The N(1)–C(4) and N(2)–C(10) bond distances of 1.295(9) and 1.27(1) Å, respectively, are indistinguishable and reflect the substantial double-bond character of each of these bonds; similarly for C(1)–C(3) 1.34(1) Å. The torsion angles of 7(1) and −5(1)° for N(1)–C(4)–C(3)–C(1) and S(1)–C(1)–C(3)–C(4), respectively, suggest the possibility of delocalisation of π-electron density across the ligand backbone. The donor atoms of L in complex **1b** are thus best described as being a thiolate S atom, a phenoxide O atom and two N atoms. The square plane about the Mn atom is not strictly planar with the deviations of S(1), O, N(1) and N(2) from the weighted least-squares plane being −0.014(2), 0.272(7), 0.221(7) and −0.258(7) Å,

Table 2 Crystallographic data for [MnL(Br)] **1b**

Formula	$C_{16}H_{18}BrMnN_2OS_2$
M	453.3
Symmetry	Monoclinic
Space group	Cc
a/Å	7.754(3)
b/Å	16.235(6)
c/Å	13.708(2)
β/°	95.73(2)
U/Å^3	1717.1(8)
Z	4
D_c/g cm^{-3}	1.753
μ/cm^{-1}	33.50
$F(000)$	912
No. unique reflections	2272
No. unique data	2121
No. of observed reflections [$I \geqslant 3\sigma(I)$]	1566
No. of parameters refined	206
R,[a] R'[b]	0.037, 0.038
ρ_{max}	0.35 e Å^{-3}

[a] $R = \Sigma(||F_o| - |F_c||)/\Sigma|F_o|$. [b] $R' = [\Sigma w(||F_o| - |F_c||)^2/\Sigma w|F_o|^2]^{\frac{1}{2}}$.

Table 3 Fractional atomic coordinates and their estimated standard deviations for [MnL(Br)] **1b**

Atom	x	y	z
Mn	−0.035 3(2)	−0.003 93(7)	0.248 8(1)
Br	0.255 7(−)	−0.017 38(6)	0.187 2(−)
S(1)	−0.251 4(3)	−0.017 0(1)	0.125 2(2)
S(2)	−0.393 5(4)	−0.140 7(1)	−0.016 9(2)
O	−0.067 5(9)	0.109 1(3)	0.236 7(4)
N(1)	−0.037 1(9)	−0.120 3(4)	0.281 5(4)
N(2)	0.031 1(9)	0.009 2(4)	0.391 2(4)
C(1)	−0.257 0(10)	−0.118 0(5)	0.088 1(6)
C(2)	−0.469 5(14)	−0.046 2(6)	−0.066 4(7)
C(3)	−0.171 8(11)	−0.181 6(5)	0.132 4(6)
C(4)	−0.073 0(10)	−0.182 8(5)	0.224 5(5)
C(5)	−0.024 1(12)	−0.268 9(4)	0.249 8(6)
C(6)	−0.042 3(12)	−0.313 1(5)	0.153 0(7)
C(7)	−0.187 9(12)	−0.268 0(5)	0.094 1(6)
C(8)	0.064 9(12)	−0.136 7(5)	0.376 2(6)
C(9)	0.036 8(13)	−0.068 4(5)	0.444 4(6)
C(10)	0.076 4(11)	0.075 7(5)	0.434 7(6)
C(11)	0.068 9(11)	0.155 5(5)	0.388 6(6)
C(12)	−0.007 2(11)	0.168 2(5)	0.293 5(6)
C(13)	−0.021 5(12)	0.248 1(5)	0.259 2(7)
C(14)	0.040 7(13)	0.311 9(5)	0.314 9(8)
C(15)	0.121 4(13)	0.298 3(5)	0.408 7(7)
C(16)	0.134 1(12)	0.222 7(5)	0.444 6(6)

respectively; the Mn atom is 0.442(1) Å above this plane in the direction of the Br atom. The two Mn–N bond distances are disparate with the shorter Mn–N(1) bond having the N(1) atom in a position approximately *trans* to the phenoxide O atom. Atom N(2) occupies a position approximately *trans* to S(1), however the angle S(1)–Mn–N(2) [147.7(2)°] deviates from the ideal 180°. This deviation may be traced in part to the restricted bite distance of the ethylenediamine chelate which constrains the N–Mn–N angle to 83.4(3)°.

The chelating ligand L forms a five- and two six-membered rings. The six-membered ring comprised of Mn, S(1), C(1), C(3), C(4) and N(1) is not planar as shown by the value of −22(1)° for the torsion angle Mn–N(1)–C(4)–C(3). Similarly, the torsion angle Mn–O–C(12)–C(11) −14(1)° indicates a significant puckering in the second six-membered ring. The conformation for the ethylenediamine ring is designated as λ. Other parameters associated with the ligand L are as expected.

Electrochemistry.—The electrochemical properties of complexes **1a**–**1d** have been investigated by cyclic voltammetry at a platinum working electrode. The experiments were carried out

Table 4 Selected interatomic distances (Å) and angles (°) for [MnL(Br)] **1b**

Mn–Br	2.497(2)	Mn–S(1)	2.271(2)
Mn–O	1.857(5)	Mn–N(1)	1.942(6)
Mn–N(2)	1.980(6)	S(1)–C(1)	1.717(9)
S(2)–C(1)	1.740(8)	S(2)–C(2)	1.76(1)
N(1)–C(4)	1.295(9)	N(1)–C(8)	1.476(9)
N(2)–C(9)	1.45(1)	N(2)–C(10)	1.27(1)
C(1)–C(3)	1.34(1)	C(3)–C(4)	1.41(1)
Br–Mn–S(1)	111.32(8)	Br–Mn–O	100.0(2)
Br–Mn–N(1)	91.2(2)	Br–Mn–N(2)	100.9(2)
S(1)–Mn–O	86.7(2)	S(1)–Mn–N(1)	93.4(2)
S(1)–Mn–N(2)	147.7(2)	O–Mn–N(1)	168.0(3)
O–Mn–N(2)	90.1(3)	N(1)–Mn–N(2)	83.4(3)
Mn–S(1)–C(1)	107.7(3)	Mn–O–C(12)	129.9(5)
Mn–N(1)–C(4)	129.0(5)	Mn–N(1)–C(8)	111.3(5)
Mn–N(2)–C(9)	113.1(5)	Mn–N(2)–C(10)	126.1(6)

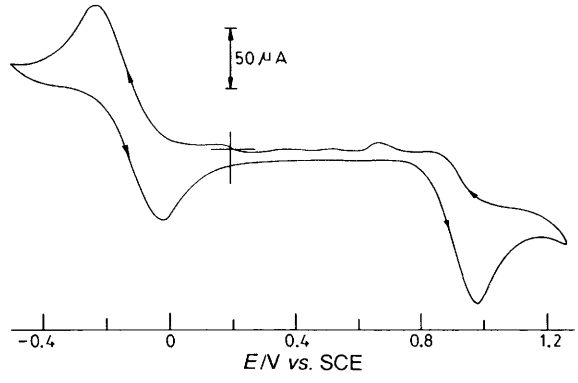

Fig. 2 Cyclic voltammogram of [MnL(Cl)] **1a** in dmf with 0.1 mol dm^{-3} NEt_4ClO_4 as supporting electrolyte (working electrode, Pt; reference electrode, SCE; scan rate, 50 mV s^{-1})

at room temperature in dmf solution using 0.1 mol dm^{-3} NEt_4ClO_4 as supporting electrolyte. Potentials were measured using either a SCE or a Ag–AgCl reference electrode but have been referred to the SCE. With the exception of **1d**, the complexes exhibit grossly identical voltammetric features independent of the axial group (X) and involve two redox processes within the potential range −1.0 to 1.5 V *vs.* SCE. The ligand H_2L is electrode inactive throughout this range. The cyclic voltammogram of **1a**, a representative example, is shown in Fig. 2 and the relevant electrochemical data are summarised in Table 5. In the cathodic range a quasi-Nernstian[37] one-electron reduction (process I) is observed for each of these complexes with associated $E_{\frac{1}{2}}$ values very close to −0.12 V. Controlled-potential coulometric experiments performed at potentials more negative than the respective E_{pc} values confirm this reduction (process I) to be monoelectronic ($n = 1.0 \pm 0.1$) involving the couple Mn^{III}–Mn^{II}.

In the anodic span an irreversible oxidation (process II) is observed with $E_{pa} \approx 1.0$ V *vs.* SCE. Failure to observe any cathodic response in this case even at a sufficiently high scan rate (500 mV s^{-1}) indicates extreme instability of the oxidised species on the voltammetric time-scale. Attempted coulometry at potentials more anodic than E_{pa} did not produce any meaningful result because of unidentified reaction(s). However, a one-electron transfer involving the couple Mn^{III}–Mn^{IV} for this oxidation process has been arrived at by comparing the current height at E_{pa} with the corresponding one-electron current parameter (E_{pc}) of process I (Fig. 2) together with the use of the appropriate equation as described elsewhere.[38] The electrochemical parameters are thus consistent with two

Table 5 Summary of electrochemical data[a] for the complexes

	Mn^{III}–Mn^{II}				Mn^{III}–Mn^{IV}
Complex	$E_{\frac{1}{2}}$[b]/mV	ΔE_p[c]/mV	i_{pc}/i_{pa}	n[d]	E_{pa}[b]/mV
1a	−120	210	1.01	0.96	980
1b	−118	200	0.93	0.92	1000
1c	−125	210	0.96	1.10	990
2a	−130	110	1.05	1.05	—
2b	−130	105	1.01	1.08	—
2c	−134	110	1.03	1.09	—

[a] Solvent dmf, supporting electrolyte NEt_4ClO_4 (0.1 mol dm^{-3}), solute concentration *ca.* 10^{-3} mol dm^{-3}, working electrode platinum. [b] Potentials are *vs.* SCE and estimated by cyclic voltammetry at a scan rate of 50 mV s^{-1}; $E_{\frac{1}{2}} = 0.5(E_{pc} + E_{pa})$. [c] $\Delta E_p = E_{pc} - E_{pa}$. [d] Number of electrons per molecule determined by controlled-potential coulometry.

successive one-electron steps involving three manganese oxidation states [equation (1)].

$$[Mn^{II}L(dmf)] \underset{\text{process I}}{\overset{+e}{\rightleftharpoons}} [Mn^{III}L(dmf)]^+ \xrightarrow[\text{process II}]{-e^-} [Mn^{IV}L(dmf)]^{2+} \quad (1)$$

The close similarity in electrochemical behaviour thus observed for complexes **1a**–**1c** in dmf (Table 5) leads us to believe that the electroactive species in each case is the same solvated $[MnL(dmf)]^+$ ion obtained by extensive anion replacement. Voltammetric experiments in a non-co-ordinating solvent, *viz.* nitrobenzene, have been also conducted to study the electron-transfer properties of **1a**–**1c** with anionic ligands (X) retained in the co-ordination sphere. Only complicated electrode processes of irreversible nature were observed which at this stage we are not confident to discuss any further. Compound **1d** is electrode inactive.

Magnetism and Electronic Spectra.—The room-temperature magnetic moments of the powdered polycrystalline samples are listed in Table 1. The observed values (4.90–4.71 μ_B) for **1a**–**1d** are in excellent agreement with the spin-only moment (4.9 μ_B) for a high-spin d^4 ($S = 2$) configuration, normally observed for mononuclear manganese(III) complexes.[39,40] No X-band EPR signal is observed with these complexes both at ambient temperature and 80 K. This is as expected[41] for high-spin ($S = 2$) manganese(III) complexes with non-Kramers spin states within which transitions are not feasible as a result of either large zero-field splittings or rapid spin-relaxation processes.

The visible spectra of the complexes have almost identical features containing multiple absorption bands mostly in the form of shoulders. A representative spectrum (**1c**) is shown in Fig. 3 and the absorption data are summarised in Table 6. In dmf solution two prominent bands, ostensibly associated with d–d transitions (ε 245–725 dm^3 mol^{-1} cm^{-1}) are observed in the 900–500 nm range [Fig. 3(*a*)] along with a high-intensity (ε *ca.* 4300–4900 dm^3 mol^{-1} cm^{-1}) band of charge-transfer origin at *ca.* 440 nm [Fig. 3(*b*)]

In the axially elongated [MnL(X)] molecules with non-cubic local symmetry (C_{4v}), as is apparent from the crystal structure of **1b**, the central manganese(III) ion will have an orbital–singlet $^5B_1$ ($d^1_{xy}, d^2_{xz,yz}, d^1_{z^2}$) electronic ground state with $^5A_1$ ($d^1_{xy}, d^2_{xz,yz}, d^1_{x^2-y^2}$), ^5E ($d^1_{xy}, d^1_{xz,yz}, d^1_{z^2}, d^1_{x^2-y^2}$) and $^5B_2$ ($d^2_{xz,yz}, d^1_{z^2}, d^1_{x^2-y^2}$) excited quintuplets appearing from lower to higher energy (Fig. 4, inset)[39,42] Consequently three spin-allowed d–d transitions $^5B_1 \longrightarrow {}^5A_1$ (I), $^5B_1 \longrightarrow {}^5E$ (II) and $^5B_1 \longrightarrow {}^5B_2$ (III) are possible in this type of system of which only one (I) will involve an electron from the d_{z^2} orbital and is thus expected

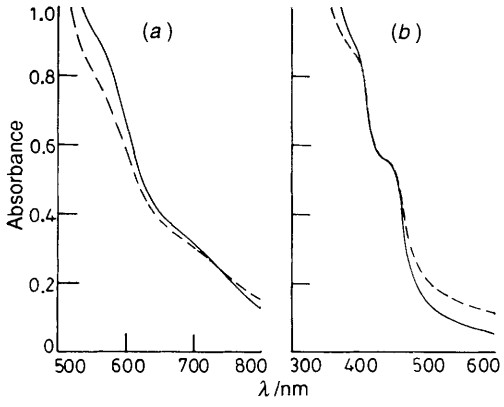

Fig. 3 Electronic spectra of [MnL(NCS)] **1c** (——) [1.42 × 10^{-3} (*a*), 1.14 × 10^{-4} mol dm^{-3} (*b*)] and $[MnL(4Me\text{-}py)]ClO_4$ **2c** (- - -) [1.01 × 10^{-3} (*a*), 1.01 × 10^{-4} mol dm^{-3} (*b*)] in dmf at ambient temperature

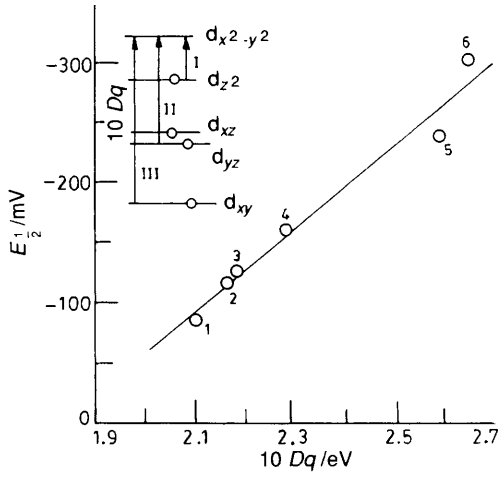

Fig. 4 Plot of 10 *Dq* ($d_{xy} \longrightarrow d_{x^2-y^2}$) *vs.* $E_{\frac{1}{2}}$ (Mn^{III}–Mn^{II}) for a series of square-pyramidal neutral $[Mn^{III}L'(NCS)]$ complexes involving tetradentate biprotic ligands (H_2L'): L' = salophen (1), salen (2), L (3), hsalpn [H_2hsalpn = 2-hydroxy-*N*,*N*′-bis(salicylidene)propane-1,2-diamine] (4), msalen (5) and acacen (6). The inset shows schematic energy levels of high-spin Mn^{III} in a crystal field of C_{4v} symmetry

to be influenced by the axial ligand. As noted in Table 6, none of the bands obtained with these compounds in dmf shows any variation with the axial anions. Perhaps an identical light-absorbing species presumably with axially co-ordinated molecule(s) of solvent is generated from each of these compounds in a co-ordinating solvent, *viz.* dmf (see above) which makes it difficult to appreciate the influence if any of ligand X on the spectra. This has prompted us to re-examine these spectra in nitrobenzene solution where [MnL(X)] compounds are known to retain their five-co-ordinated structure with ligand X in the axial position (see above). Measurement in this solvent below 450 nm is not reliable because of some disturbances. Nevertheless, two d–d transitions are observed in the 900–500 nm region (ε 284–820 dm^3 mol^{-1} cm^{-1}) with features slightly shifted to longer wavelengths but not affected by the axial ligands. Similar invariance with group X has been observed in the solid state (Nujol mull) for two representative compounds (**1a**, **1d**) as shown in Table 6. We are thus inclined to assign the low-energy d–d band centred at *ca.* 685 nm to the $^5B_1 \longrightarrow {}^5E$ transition and that at higher energy (570 nm) to the $^5B_1 \longrightarrow {}^5B_2$ transition. For square-pyramidal complexes such as **1a**–**1d** the energy of the latter band involving a $d_{xy} \longrightarrow d_{x^2-y^2}$ electronic excitation (Fig. 4, inset) is a direct measure of the ligand-field strength (10 *Dq*) as the metal d_{xy} orbital here would be of

Table 6 Electronic spectral data for the complexes

Complex	Medium	λ_{max}/nm (ε/dm^3 mol^{-1} cm^{-1})
1a	dmf	682(298), 564(710), 438(4325), 393(7650)
	Nitrobenzene	690(370), 572(745)
	Nujol mull	693, 577, 440, 394
1b	dmf	683(312), 567(725), 441(4370), 382(7400)
	Nitrobenzene	690(284), 569(783)
1c	dmf	684(245), 560(633), 440(4900), 394(7800)
	Nitrobenzene	694(380), 569(820)
1d	dmf	678(322), 563(635), 442(4700), 393(5470)
	Nitrobenzene	690(284), 569(785)
	Nujul mull	692, 570, 443, 390
2a	dmf	690(338), 570(683), 440(4330), 390(8100)
2b	dmf	690(324), 560(633), 445(3980), 390(7800)
2c	dmf	690(315), 560(780), 440(5460), 390(8580)

Table 7 Electrochemical[a] and spectroscopic[b] data for square-pyramidal manganese(III) complexes [MnL'(NCS)] containing biprotic tetradentate ligands

Complex	$E_{\frac{1}{2}}$[a] (Mn^{III}–Mn^{II})/mV	$10Dq$[b] ($d_{xy} \longrightarrow d_{x^2-y^2}$)/eV
[Mn(salophen)(NCS)]	−86	2.10
[Mn(salen)(NCS)]	−117	2.16
[MnL(NCS)]	−125	2.18
[Mn(hsalpn)(NCS)]	−160[c]	2.29[d]
[Mn(msalen)(NCS)]	−238	2.59
[Mn(acacen)NCS]	−302	2.64

[a] All potentials were measured by cyclic voltammetry (50 mV s^{-1} scan rate) using a platinum working electrode in dmf–0.1 mol dm^{-3} NEt_4ClO_4 *vs.* SCE, unless otherwise mentioned. [b] Spectra recorded in dmf. [c] Ref. 43. [d] Ref. 44.

appropriate symmetry to interact effectively with the basal donor atoms of the quadridentate ligand which contribute an average in-plane ligand field. Consequently, the energy is expected to be sensitive towards the in-plane donor strength of the quadridentate ligands as shown in Table 7 for the present and related manganese(III) complexes. For comparison we have only included the complexes where thiocyanate serves as the axial anion because of their ease of preparation in the pure form. The observed order in $10Dq$ is salophen < salen < L < hsalpn < msalen < acacen.

The complexes exhibit two charge-transfer bands [Fig. 3(*b*)] in the near-UV region. That at *ca.* 440 nm (Table 6) may be attributable to phenolate oxygen-based ligand-to-metal charge transfer (l.m.c.t.) O (p_π)→Mn (d_{π^*}) by analogy with related manganese(III) complexes.[43,45] The remaining band at *ca.* 390 nm is most likely due to S→Mn^{III} c.t.[46] and/or to a ligand internal π–π^* transition.[25] The unique spectral feature of the manganese(III) centre in purple acid phosphatase is the appearance of a c.t. band at 515 nm (ε 2460 dm^3 mol^{-1} cm^{-1}) tentatively assigned[19] as due to tyrosine (O)→Mn^{III} or/and cysteine (S)→Mn^{III} charge transfer(s), thus suggesting the presence of a tyrosine phenolate or/and cysteine thiolate anion(s) in the active site locus of the proposed mononuclear manganese(III) centre. Unfortunately the present five-co-ordinated manganese(III) complexes, notwithstanding the presence of a N_2OS donor assembly comprising both phenolate oxygen and thiolate sulfur,† fail to exhibit any comparable charge-transfer band in the visible region.

† The carbodithioate sulfur of co-ordinated L behaves more like an electronic analogue of thiolate sulfur as confirmed by the crystal structure of complex **1b**. The C–S bond distance is comparable to those reported for several manganese(III) thiolate complexes.[46]

Spectral and Electrochemical Correlations.—From the sequence of energy levels for a tetragonally elongated manganese(III) complex in C_{4v} symmetry[39,42] (Fig. 4, inset), the $d_{x^2-y^2}$ appears to be the highest-lying metal orbital. The extent to which this orbital is destabilised in such compounds depends on the in-plane donor strength ($10Dq$) of the tetradentate ligand, an indication of which can be obtained from the energy of the $^5B_1 \longrightarrow {}^5B_2$ transition (see above). As shown in Table 7, this energy gap ($10Dq$) changes as the ligand structure is varied within a group of square-pyramidal neutral manganese(III) complexes of grossly identical structure.‡ Since electrochemical reduction of these complexes is a metal-based process involving addition of an electron to the highest-lying metal orbital, the measured $E_{\frac{1}{2}}$ value for the Mn^{III}–Mn^{II} reduction in this case will also reflect the energy of the $d_{x^2-y^2}$ orbital. As seen from the data in Table 7, the $E_{\frac{1}{2}}$ value is most negative for the complex [Mn(acacen)(NCS)] for which the $d_{xy} \longrightarrow d_{x^2-y^2}$ band gap is maximal. While there is generally a more negative shift in $E_{\frac{1}{2}}$ value with increasing $10Dq$ of the complex, a more explicit pattern becomes apparent from a plot of $E_{\frac{1}{2}}$ against $10Dq$. An excellent linear fit (Fig. 4) with high correlation coefficient (r = 0.97) is obtained [equation (2)], thus confirming the effect due

$$E_{\frac{1}{2}} = 349.15(10Dq) - 641.02 \quad (2)$$

to ligand-field stabilisation to be dominating[47] for these neutral manganese(III) complexes of grossly identical square-pyramidal structure involving tetradentate biprotic ligands.

[MnL(B)]ClO_4 *Complexes* **2a**–**2c**.—These compounds are obtained as dark brown crystalline solids in fairly good yields (40–50%) when a suspension of **1a** in acetonitrile is treated with the stoichiometric amount of $AgClO_4$ in the presence of the required base (B), added in excess. They are air-stable solids, having reasonably good solubilities in acetonitrile, CH_2Cl_2 and dmf. In solution the compounds are 1:1 electrolytes (Table 1) and retain their identity for several hours without showing any sign of decomposition. The initial motive behind this synthesis was to achieve a more realistic combination of donor atoms as proposed[19,48] for the manganese biosite in purple acid phosphatase. Determination of the structure by X-ray crystallography was, however, not possible because of our failure to get diffraction-quality crystals of these compounds.

The IR spectra of complexes **2a**–**2c** have essentially the same features as those described for **1a**–**1d**. In addition these complexes exhibit an intense, broad absorption centred at 1080 cm^{-1} and a strong sharp band at 620 cm^{-1} which are typical for ionic perchlorate. They have spin-only moments (S = 2) at room temperature in the solid state (Table 1). Their electronic spectra in dmf have features almost identical with those reported for **1a**–**1d** (Table 6) suggesting that they all have the same electronic ground state. A representative spectrum (**2c**) is shown in Fig. 3 which displays the d–d transitions at 690 ($^5B_1 \longrightarrow {}^5E$) and 560 nm ($^5B_1 \longrightarrow {}^5B_2$) regions [Fig. 3(*a*)] expected under approximate C_{4v} symmetry (see above). Of particular interest is the presence of the nitrogen-containing base (B) in the apical position of **2a**–**2c** which apparently has no influence on the energy levels of their absorption manifold. The complexes also show a couple of intense bands (ε 3980–8580 dm^3 mol^{-1} cm^{-1}) at 440 and 390 nm [Fig. 3(*b*)] the positions of which also remain invariant with the axial ligands being changed from py (**2a**) to 4Me-py (**2c**). By analogy to our earlier

‡ For comparison we prepared several known manganese(III) complexes, *viz.* [Mn(acacen)(NCS)], [Mn(salen)(NCS)], [Mn(msalen)-(NCS)] and [Mn(salophen)(NCS)] following the same procedure (method A) we used for [MnL(NCS)]. Their electronic spectra and cyclic voltammograms were recorded in dmf under identical experimental conditions to get a reliable correlation. Spectral[44] and electrochemical[43] data for [Mn(hsalpn)(NCS)] were taken from the literature.

interpretation (for **1a**–**1d**) we ascribe the first band (at 440 nm) to O (p_π)→Mn^{III} charge transfer while S→Mn^{III} c.t. or/and a ligand internal transition could be the origin for the other band.

Cyclic voltammograms of complexes **2a**–**2c** have been recorded in dmf solution under identical conditions to those described for **1a**–**1c**. A quasi-reversible one-electron reduction, equation (3), which conforms to the formation of the

$$[Mn^{III}L(B)]^+ \overset{+e^-}{\rightleftharpoons} [Mn^{II}L(B)] \quad (3)$$

corresponding manganese(II) species (established by coulometry), is obtained in each case. Variation of the basicity of the axial ligand B does not appear to have any noticeable effect on the measured $E_{\frac{1}{2}}$ values (Table 5). A comparison of the Mn^{III}–Mn^{II} redox potentials of these positively charged complexes with those of neutral **1a**–**1c** (Table 5) reveals that the axial ligands (B) in **2a**–**2c** with large basicities have only marginal influence on the stability of manganese in +III oxidation state. These complexes unlike **1a**–**1c** do not undergo any electrochemical Mn^{III}–Mn^{IV} oxidation.

Conclusion

The mononuclear manganese(III) complexes reported here are stable at room temperature and have the required combination of phenoxo oxygen, thiolate sulfur and nitrogen atoms in the ligand donor set in order to be a realistic model for the proposed manganese(III) biosite in purple acid phosphatase.[19,48] Their electronic spectra have multiple absorption features which include a couple of high-intensity bands in the near-UV region. The characteristic band at 515 nm, observed for purple acid phosphatase, tentatively assigned as due to S→Mn^{III} charge transfer, is apparently missing for these complexes. Gohdes and Armstrong[21] did not observe such a band for an analogous manganese(III) compound containing both phenoxo oxygen and thiolate sulfur bound to the metal centre. These results along with some previous observations[21,23] clearly indicate the appearance of c.t. band(s) in the near-UV region whenever phenoxide oxygen is bound to the manganese(III) centre. This obviously imposes a question-mark about the simultaneous occurrence of thiolate sulfur and phenoxide oxygen as possible donors to the manganese active site as proposed in purple acid phosphatase.[19] Further work is indeed needed to enhance our understanding of this manganese biochromophore.

Acknowledgements

We gratefully acknowledge support of this work by the Council of Scientific and Industrial Reasearch, New Delhi [Grant No. 1(1179)/90-EMR-II] and thank Professor K. Nag for many helpful discussions and facilities for electrochemical measurements. The Australian Research Council is thanked for the support of the crystallographic facility.

References

1 K. Wieghardt, *Angew. Chem., Int. Ed. Engl.*, 1989, **28**, 1153; G. Christou, *Acc. Chem. Res.*, 1989, **22**, 328; V. L. Pecoraro, *Photochem. Photobiol.*, 1988, **48**, 249; G. Brudvig and R. H. Crabtree, *Prog. Inorg. Chem.*, 1989, **37**, 99; Jr. L. Que and A. E. True, *Prog. Inorg. Chem.*, 1990, **38**, 97.
2 K. Sauer, *Acc. Chem. Res.*, 1980, **13**, 2249; Govindjee and W. Coleman, *Sci. Am.*, 1990, **262**, 50; G. Renger, *Angew. Chem., Int. Ed. Engl.*, 1987, **26**, 643.
3 Jr. W. F. Beyer and I. Fridovich, *Biochemistry*, 1985, **24**, 6460; Y. Kono and I. Fridovich, *J. Biol. Chem.*, 1983, **258**, 6015.
4 I. Fridovich, *Acc. Chem. Res.*, 1982, **115**, 2200; J. S. Vallentine and D. MotadeFreitas, *J. Chem. Educ.*, 1985, **62**, 990.
5 G. N. George, R. C. Prince and S. P. Cramer, *Science*, 1989, **243**, 789; J. E. Penner-Hahn, R. M. Fronko, V. L. Pecoraro, C. F. Yocum, S. D. Betts and N. R. Bowlby, *J. Am. Chem. Soc.*, 1990, **112**, 2549; G. S. Waldo, S. Yu and J. E. Penner-Hahn, *J. Am. Chem. Soc.*, 1992, **114**, 5869; D. H. Kim, R. D. Britt, M. P. Klein and K. Sauer, *J. Am. Chem. Soc.*, 1990, **112**, 9389; V. K. Yachundra, R. D. Guiles, K. Sauer and M. P. Klein, *Biochim. Biophys. Acta*, 1986, **850**, 333.
6 N. Kitajima, M. Osawa, N. Tamura, Y. Moro-oka, T. Hirano, M. Hirobe and T. Nagano, *Inorg. Chem.*, 1993, **22**, 1879.
7 C. P. Horwitz, P. J. Winslow, J. T. Warden and C. A. Lisek, *Inorg. Chem.*, 1993, **32**, 82.
8 E. Larson, A. Haddy, M. L. Kirk, R. H. Sands, W. E. Hatfield and V. L. Pecoraro, *J. Am. Chem. Soc.*, 1992, **114**, 6263.
9 S. Pal, M. K. Chan and W. H. Armstrong, *J. Am. Chem. Soc.*, 1992, **114**, 6398.
10 S.-B. Yu, S. J. Lippard, I. Shweky and A. Bino, *Inorg. Chem.*, 1992, **31**, 3502.
11 R. Manchanda, H. Holden Thorp, G. W. Brudvig and R. H. Crabtree, *Inorg. Chem.*, 1992, **31**, 4040.
12 U. Bossek, M. Saher, T. Weyhermuller and K. Wieghardt., *J. Chem. Soc., Chem. Commun.*, 1992, 1780.
13 E. J. Larson and V. L. Pecoraro, *J. Am. Chem. Soc.*, 1991, **113**, 7809.
14 E. J. Larson and V. L. Pecoraro, *J. Am. Chem. Soc.*, 1991, **113**, 3810.
15 Y. Naruta and K. Maruyama, *J. Am. Chem. Soc.*, 1991, **113**, 3595.
16 J. S. Bashkin, H. R. Chang, W. E. Streib, J. C. Huffman, D. N. Hendrickson and G. Christou, *J. Am. Chem. Soc.*, 1987, **109**, 6502.
17 P. Mathur, M. Crowder and G. C. Dismukes, *J. Am. Chem. Soc.*, 1987, **109**, 5227.
18 F. M. Ashmawy, C. A. McAuliffe, R. V. Parish and J. Tames, *J. Chem. Soc., Dalton Trans.*, 1985, 1391.
19 H. Kawabe, Y. Sugiura, M. Terauchi and H. Tanaka, *Biochim. Biophys. Acta*, 1984, **784**, 81; Y. Sugiura, H. Kawabe, H. Tanaka, S. Fujimoto and A. Ohara, *J. Biol. Chem.*, 1981, 256, 10664; Y. Sugiura, H. Kawabe, H. Tanaka, S. Fujimoto and A. Ohara, *J. Am. Chem. Soc.*, 1981, **103**, 963; Y. Sugiura, H. Kawabe and H. Tanaka, *J. Am. Chem. Soc.*, 1980, **102**, 6581.
20 S. K. Hefler and B. A. Averill, *Biochim. Biophys. Res. Commun.*, 1987, **146**, 1173.
21 J. W. Gohdes and W. H. Armstrong, *Inorg. Chem.*, 1988, **27**, 1841.
22 J. S. Bashkin, J. C. Huffman and G. Christou, *J. Am. Chem. Soc.*, 1986, **108**, 5038.
23 S. B. Kumar and M. Chaudhury, *J. Chem. Soc., Dalton Trans.*, 1992, 3439.
24 S. K. Dutta, S. B. Kumar, S. Bhattacharyya and M. Chaudhury, *J. Chem. Soc., Dalton Trans.*, 1994, 97; S. B. Kumar and M. Chaudhury, *J. Chem. Soc., Dalton Trans.*, 1992, 269; 1991, 2169, 1149 and refs. therein.
25 S. K. Mondal, P. Paul, R. Roy and K. Nag, *Transition Met. Chem. (Weinheim, Ger.)*, 1984, **9**, 247.
26 R. D. Bereman, M. W. Churchill and G. D. Shields, *Inorg. Chem.*, 1979, **18**, 3117; E. M. Martin, R. D. Bereman and P. Singh, *Inorg. Chem.*, 1991, **30**, 957.
27 H. Lux, in *Handbook of Preparative Inorganic Chemistry*, 2nd edn., ed. G. Brauer, Academic Press, New York, 1965, vol. 2, p. 1469.
28 B. R. Stults, R. S. Marianelli and V. W. Day, *Inorg. Chem.*, 1975, **14**, 722.
29 D. D. Perrin, W. L. F. Armarego and D. R. Perrin, *Purification of Laboratory Chemicals*, 2nd edn., Pergamon, Oxford, 1980.
30 TEXSAN Structure Analysis Software, Molecular Structure Corporation, Houston, TX, 1985.
31 N. Walker and D. Stuart, *Acta Crystallogr., Sect. A*, 1983, **39**, 158.
32 G. M. Sheldrick, SHELXS 86, Program for the Automatic Solution of Crystal Structure, University of Göttingen, 1986.
33 C. K. Johnson, ORTEP, Report ORNL-5138, Oak Ridge National Laboratory, Oak Ridge, TN, 1976.
34 R. A. Bailey, S. L. Kozak, T. W. Michelsen and W. N. Mills, *Coord. Chem. Rev.*, 1971, **6**, 407.
35 Z. Dori and R. F. Ziolo, *Chem. Rev.*, 1973, **73**, 247; R. Vicente, A. Escuer, J. Ribas, M. S. el Fallah, X. Solans and M. Font-Bardia, *Inorg. Chem.*, 1993, **32**, 1920.
36 W. J. Geary, *Coord. Chem. Rev.*, 1971, **7**, 81.
37 R. S. Nicholson and I. Shain, *Anal. Chem.*, 1964, **36**, 706.
38 M. Chaudhury, *Inorg. Chem.*, 1984, **23**, 4434.
39 B. J. Kennedy and K. S. Murray, *Inorg. Chem.*, 1985, **24**, 1552.
40 H.-R. Chang, S. K. Larson, P. D. W. Boyd, C. G. Pierpont and D. N. Hendrickson, *J. Am. Chem. Soc.*, 1988, **110**, 4565; D. V. Behere and S. Mitra, *Inorg. Chem.*, 1980, **19**, 992.
41 S. L. Dexheimer, J. W. Gohdes, M. K. Chan, K. S. Hagen,

W. H. Armstrong and M. P. Klein, *J. Am. Chem. Soc.*, 1989, **111**, 8923.
42 L. B. Dugad, D. V. Behere, V. R. Marathe and S. Mitra, *Chem. Phys. Lett.*, 1984, **104**, 353.
43 J. A. Bonadies, M. J. Maroney and V. L. Pecoraro, *Inorg. Chem.*, 1989, **28**, 2044.
44 K. Bertoncello, G. D. Fallon and K. S. Murray, *Inorg. Chem.*, 1991, **30**, 3562.
45 A. Neves, S. M. D. Erthal, I. Vencato, A. S. Ceccato, Y. Mascarenhas, O. R. Nascimento, M. Horner and A. A. Batista, *Inorg. Chem.*, 1992, **31**, 4749.
46 T. Costa, J. R. Dorfman, K. S. Hagen and R. H. Holm, *Inorg. Chem.*, 1983, **22**, 4091.
47 F. P. Bossu, K. L. Chellappa and D. W. Margerum, *J. Am. Chem. Soc.*, 1977, **99**, 2195.
48 S. Fujimoto, K. Murakami and A. Ohara, *J. Biochem.*, 1985, **97**, 1777.

Received 9*th February* 1995; *Paper* 5/00783F